ICSO 2016

International Conference on Space Optics

Biarritz, France

18–21 October 2016

Edited by Bruno Cugny, Nikos Karafolas and Zoran Sodnik

Investigation of coherent receiver designs in high-speed optical inter-satellite links using digital signal processing

S. Schaefer

M. Gregory

W. Rosenkranz

esa icso proceedings cnes

International Conference on Space Optics — ICSO 2016, edited by Bruno Cugny, Nikos Karafolas, Zoran Sodnik, Proc. of SPIE Vol. 10562, 1056251 · © 2016 ESA and CNES
CCC code: 0277-786X/17/$18 · doi: 10.1117/12.2296112

INVESTIGATION OF COHERENT RECEIVER DESIGNS IN HIGH-SPEED OPTICAL INTER-SATELLITE LINKS USING DIGITAL SIGNAL PROCESSING

S. Schaefer[1], M. Gregory[2], W. Rosenkranz[1]
[1]*Christian-Albrechts-Universität zu Kiel, Chair for Communications, Kaiserstraße 2, D-24143 Kiel, Germany*
[2]*TESAT-Spacecom GmbH & Co.KG, Gerberstraße 49, D-71522 Backnang, Germany*
sesc@tf.uni-kiel.de

I. INTRODUCTION

Due to higher data rates, better data security and unlicensed spectral usage optical inter-satellite links (OISL) offer an attractive alternative to conventional RF-communication. However, the very high transmission distances necessitate an optical receiver design enabling high receiver sensitivity which requires careful carrier synchronization and a quasi-coherent detection scheme. In state of the art systems a homodyne detection scheme uses an optical phase-locked loop (OPLL), to adjust the frequency and phase of the local laser to the incoming signal [1,2]. However, the OPLL hardware complexity increases with the modulation order. Therefore, we propose an intradyne detection scheme, where the local laser at the receiver runs un-synchronized and frequency offset and phase noise compensation is done by digital signal processing (DSP) after the optical front end. Since software-based coherent detection is very flexible, several space applications are possible. Next to the conventional LEO to GEO optical high speed transmissions, low distance LEO to LEO links with high order modulation formats are imaginable as well.
In fact, DSP-based coherent detection is well-known in fiber communications for many years. In the 1990s intradyne detection with a digital receiver realization was first proposed [3]. Typically, the digital frequency offset and phase noise compensation are based on a feedforward carrier recovery [4] and on the phase estimation algorithms by Viterbi & Viterbi [5], which are used in today's high-end long distance terrestrial fiber optic receivers and are also part of this work.
This paper presents simulative and experimental investigations of homodyne and intradyne detection schemes for high-order modulation formats in optical inter-satellite communication systems. We focus on intradyne detection which is based on software-defined digital frequency offset and phase noise compensation and compare different compensation algorithms in a 2-, 4- and 8-PSK OISL transmission system. We explain the applied algorithms and present simulative and experimental results in terms of receiver sensitivity and bit error ratio (BER). Finally, we compare our intradyne approach with the OPLL based homodyne detection and show that digital frequency offset and phase noise compensation is a promising solution in OISL for increasing the data rate and system flexibility.

II. DIGITAL DOPPLER FREQUENCY-SHIFT COMPENSATION

Doppler-shift occurs due to the relative velocity between the satellites which will shift the optical carrier frequency up to ±7 GHz. Since the altitude and velocity of the satellites are known, the frequency shift can be predetermined and the frequency of the lasers can be adjusted in real-time by using known trajectory data. Usually, a small frequency offset (FO) remains, which is conventionally compensated for by an OPLL. However, its structure is related to the modulation format, which increases in complexity when increasing the modulation order. Therefore, in order to achieve a more flexible system, we propose a software-based intradyne detection scheme in OISL.
As seen in the proposed OISL system depicted in Fig. 1 the sampled input signal to the DSP is

$$\begin{aligned} X[k] &= I[k] + jQ[k] \\ &= \hat{A} e^{j\left(\Delta\phi[k] + \phi_M[k] + \phi_0 + \phi_{\mathrm{PN}}[k]\right)} + \underline{n}[k], \end{aligned} \tag{1}$$

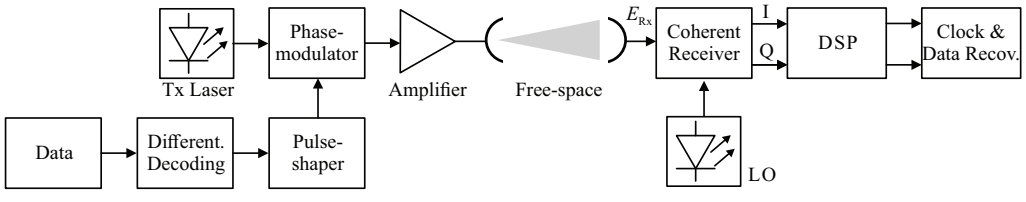

Fig. 1. BPSK OISL transmission system

where $\hat{A}$ denotes the intensity of the coherently detected signal, $\Delta\phi$ the phase drift due to the frequency offset f_{FO}, ϕ_M the data modulation, ϕ_0 a constant phase offset, ϕ_{PN} the phase noise and $\underline{n}[k]$ the (complex) additive noise.

Since phase and shot noise are the main dominating noise sources a phase noise compensation (PNC) stage is required. This fine compensation is usually based on the Viterbi & Viterbi algorithm. This method considers the average absolute phase value of N samples,

$$\tilde{\Phi}[k] = \frac{1}{M}\arg\left\{\sum_{n=k+1}^{k+N}\left(Y[n]\right)^M\right\}. \tag{2}$$

If $Y[k] = \mathrm{X}[k]$ is assumed to be the input to the fine compensation, the resulting output is

$$Z[k] = Y[k]\cdot\exp\left(-j\tilde{\Phi}[k]\right). \tag{3}$$

In a first step we investigate the ability of the phase noise compensation stage to compensate for the frequency offset as well. In Fig. 2 (left) the simulated BER for different offsets and averaging lengths are considered. We can observe that the PNC is able to compensate for only small offsets up to several MHz. Hence, using this fine compensation can compensate the frequency offset only in a small range. In order to increase the compensation range we need an additional coarse frequency offset compensation (FOC) stage before. Digital FOC consists of two steps, estimation and compensation. In the following we describe three different algorithms for frequency offset estimation.

A. Phase Differential Algorithm (PDA)

The PDA describes the typical feedforward carrier recovery. By multiplying two consecutive samples we get the phase difference and applying the power of M will eliminate the modulation ϕ_M,

$$\Gamma[k] = \left(X[k]\cdot X^*[k-1]\right)^M, \tag{4}$$

where M denotes the modulation order for M-PSK. If neglecting the noise Eq. (1) results in

$$\Gamma[k] = \hat{A}^{2M}\cdot e^{jM\left(\Delta\phi[k]-\Delta\phi[k-1]\right)}. \tag{5}$$

The final estimated frequency offset is based on the moving average of L samples,

$$\Delta f_{est}[k] = \frac{1}{2\pi T_s M}\cdot\arg\left\{\sum_{v=k+1}^{k+L} w[v]\cdot\Gamma[v]\right\} \text{ and } w[v]=1, \tag{6}$$

where T_S denotes the sampling period and arg{} the phase extraction function. Due to the $\pm\pi$ restriction of the arg{}-operation the maximum frequency offset which can be compensated for is calculated by, $\Delta f_{\max,\min} = \pm 1/2MT_s$.

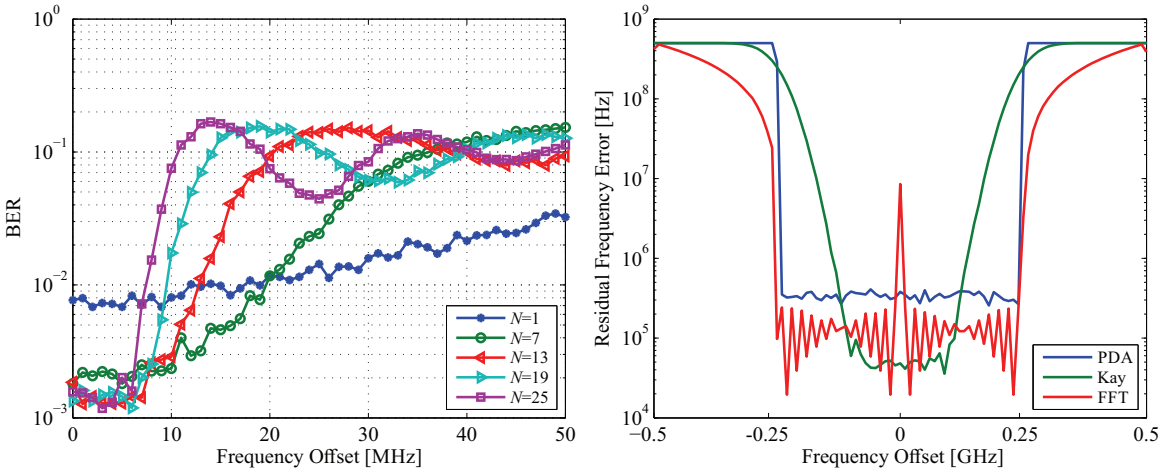

Fig. 2. Investigation of PNC (left), and FOC (right) with L=1024

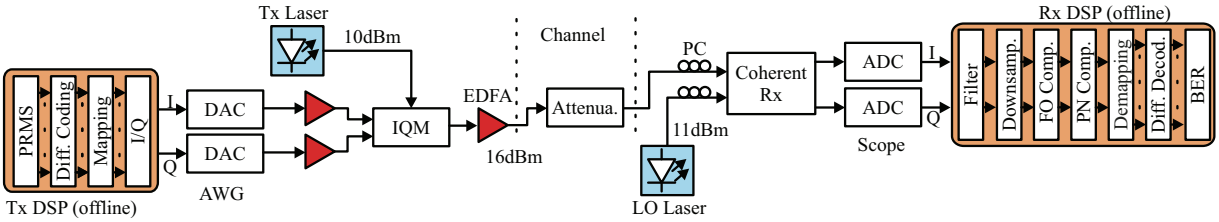

Fig. 3. Experimental setup of the intradyne transmission system with emulated free-space channel.

B. Kay-Estimator

Similar to the PDA a least-square based estimator was proposed by [7] and [8]. Main difference to the PDA are the weighted coefficients $w[k]$,

$$w[k] = \frac{6k(L-k)}{L(L^2-1)}, \text{ with } 1 \le k \le L-1. \tag{7}$$

As seen on the right side in Fig. 2 this leads to a slightly better estimation accuracy. However, the estimation range decreases.

C. FFT-Algorithm

In case of the previous two methods a data-free signal is required, achieved by applying the power of *M*. The following FFT-based algorithm is independent of the data signal [8, 9]. The phase of the *k*-th sample is,

$$\begin{aligned} \Phi[k] &= \arg\{X[k]\} = \Delta\phi[k] + \phi_M[k] + \phi_0 + \phi_{\mathrm{PN}}[k] \\ &= 2\pi f_{\mathrm{FO}} k T_s + \phi_M[k] + \phi_0 + \phi_{\mathrm{PN}}[k] \ , \end{aligned} \tag{8}$$

and the frequency offset is finally estimated by applying the FFT with length *L* and detecting the peak frequency component,

$$\Delta f_{\mathrm{est}} = \frac{1}{M}\left\{ f = \max\left(\mathrm{FFT}\{\Phi[k]\}\right)\right\} \text{ with } 1 \le k \le L \ . \tag{9}$$

After frequency offset estimation, the compensation is applied. If $X[k]$ is assumed to be the input to the coarse compensation, the resulting output is

$$Y[k] = X[k] \cdot \exp\left(-j2\pi f_{\mathrm{est},k} k T_s\right). \tag{10}$$

All following investigations are based on the PDA algorithm together with phase noise compensation by Viterbi & Viterbi.

III. SIMULATIVE AND EXPERIMENTAL SETUP

Figure 3 shows the simulative and experimental setup for *M*-PSK transmission with intradyne detection. The data generation is done offline in Matlab containing a pseudo random multilevel sequence (PRMS) of length 2^{23} and differential decoding in order to avoid errors due to cycle slips. After mapping, the data symbols are fed to the arbitrary waveform generator (AWG) for digital-to-analog-conversion (DAC). The light from Tx laser is externally modulated by an IQ-Modulator (IQM). The output signal is amplified by an erbium doped fiber amplifier (EDFA) to 16 dBm and finally coupled into the channel. The free-space channel is emulated by an attenuator. The received optical signal is detected by the coherent receiver front end. We use polarization controllers (PC) in order to shift the light in only one polarization so that the received power is maximized. The receiver contains a 90° optical hybrid, which superimposes the receive light with the LO light. This setup will be termed as "hybrid-homodyne" throughout the rest of the paper, in contrast to the true homodyne detection based on a 3 dB coupler with balanced detection. The resulting I- and Q-signals are converted to the electrical domain by photodiodes (PD) and amplified by transimpedance amplifiers (TIA). After ADC (50 GSamples/s) the signal is forwarded into the DSP, i.e. in our case to the offline processing with Matlab. Here, the signal is filtered, further down-sampled to one sample per symbol and processed by the two presented compensation stages. After demapping and differential decoding we finally get the received bits. The system parameters are given in Table 1. In order to emulate the link distance between the satellites, the Rx power is varied by changing the attenuation. As in a real OISL system we assume that the Doppler-shift has already been pre-compensated, as described before by using the trajectory data, and therefore we only consider the final residual FO. We manually set this FO by

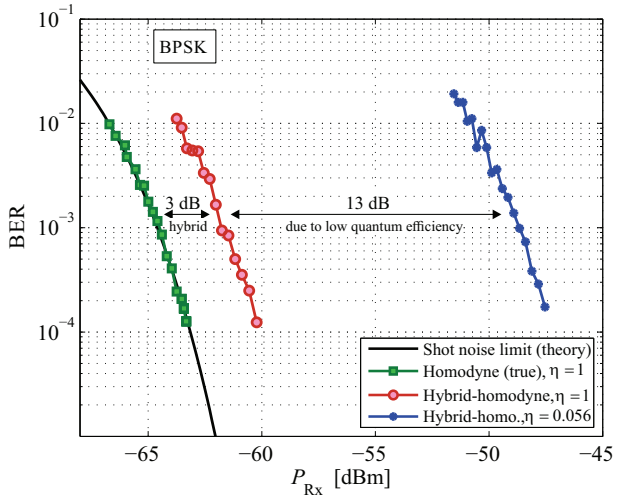

Fig. 4. Influence of the PD quantum efficiency

coarse detuning the LO at the receiver side, here in the range between $f_{FO} = 50$ to 100 MHz. For later comparison we additionally change our detection scheme in the experiments to quasi-homodyne, i.e. we use the same setup but with a single laser as Tx laser and LO. Main advantage of the software-based intradyne detection compared to OPLL based hybrid-homodyne detection is the easy adaptation to different modulation formats. For example, by simply changing the modulation order to $M = 4$, the receiver is able to detect QPSK signals as well. The DSP complexity remains constant. Typically in current OISL systems the laser linewidth is very narrow (some kHz). In our setup we use DFB lasers at 1550 nm with laser linewidth smaller than 10 kHz. The data rate in practical optical communication systems is mainly limited by electronic devices, e.g. DAC/ADC bandwidth, and since space-qualified DSP for OISL is much slower, we set the symbol rate to 1 GS/s in order to get a more realistic scenario. Current OISL systems achieve data rates between 1 to 6 Gbps [1, 2]. Our simulation setup is similar to the experimental setup. However, instead of quasi-homodyne we use OPLL based hybrid-homodyne detection.

IV. RESULTS

Figure 4 compares the simulated model to theory. As already mentioned in Sec. II, shot and thermal noise are the main noise sources in OISL, whereas due to the high LO power shot noise is dominating. According to theory the BER for a shot noise limited system based on a quantum efficiency of

$$\eta = \frac{R \cdot hf}{q} = 1 \text{ (Quantum limit)}, \tag{11}$$

can be calculated by

$$\text{BER} = \frac{1}{2} erfc\left(\sqrt{\frac{2P_{Rx}T_b}{hf}}\right), \tag{12}$$

Table 1 System parameters.

Tx power	P_{Tx}	16 dBm
DAC symbol rate	f_s	1 GS/s
Rx power range	P_{Rx}	-44 to -30 dBm
Rx filter (Butterw.5th or.)	B_{Rx}	1 GHz
PD responsivity	R	0.07 A/W
PN compen. filter length	N	16
FO compen. filter length	L	256
Residual FO (intradyne)	f_{FO}	100 MHz
LO power	P_{LO}	12 dBm
Linewidth (Tx/Rx)	$\Delta\nu$	<10 kHz

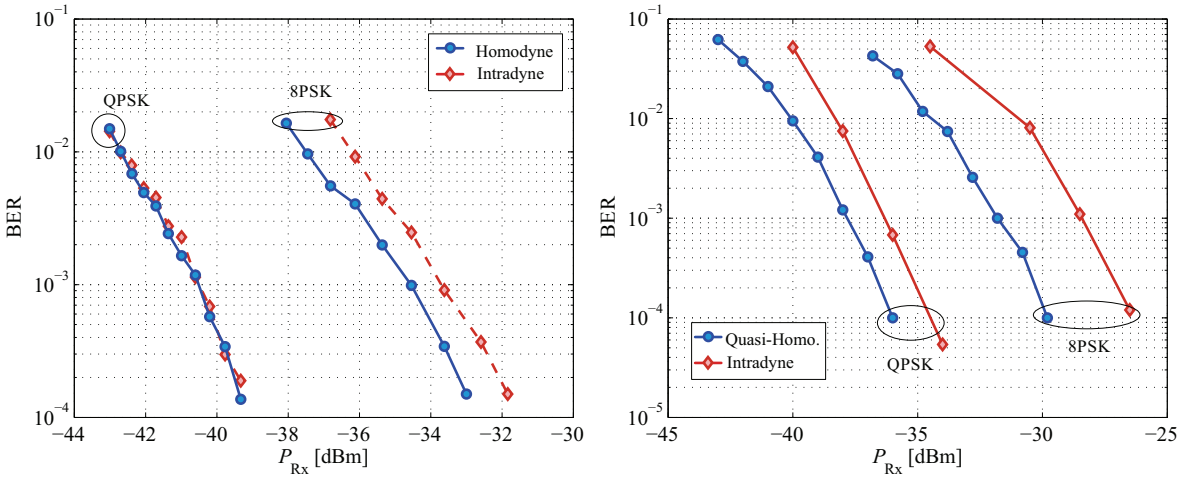

Fig. 5. (Quasi-)Homodyne and intradyne detection: simulation (left), measurement (right)

where q denotes the elementary charge with $q = 1.6021 \cdot 10^{-19}\,\mathrm{C}$, h the Planck constant with $h = 6.626 \cdot 10^{-34}\,\mathrm{Js}$, f the optical frequency, R the PD responsivity, P_{Rx} the received optical power and T_{b} the bit duration. Since differential decoding is applied, the BER in (12) is doubled due to the error propagation in the decoder.

The theoretical curve in Fig. 4 shows a receiver sensitivity of approx. –64 dBm or 3 photons per bit at BER=10^{-3} in case of BPSK with matched filtering and 1550 nm wavelength. The green curve in Fig. 4 validates this. However, several impacts can impair the sensitivity but which are mostly depending on the used lab equipment. By using the 90° hybrid and equally splitting the power into I and Q we lose 3 dB, since the shot noise limit calculation for BPSK is based on a true homodyne setup with coupler and balanced detection instead. The poor quantum efficiency of the lab photodiode ($\eta = 0.056$) will further decrease the sensitivity by approx. 13 dB to -48 dBm. However, modern photodiodes achieve an efficiency of $\eta \approx 1$.

Figure 5 (left) shows the simulated BER versus the optical received input power in case of QPSK and 8PSK for hybrid-homodyne and intradyne detection. The simulative investigation confirms our analysis, which shows the same behavior of hybrid-homodyne and intradyne detection. Only in case of 8PSK we observe a penalty of approx. 1 dB. However, this is rather based on the inaccuracy of the FO and PN estimation than on the complex IF compensation. Compared to the hybrid-homodyne case in Fig. 4 (blue curve) we can further observe a difference of 7 dB. This difference contains the expected 3 dB penalty in the optical received power in case of QPSK since the data rate changes from 1 Gb/s to 2 Gb/s. The remaining 4 dB losses are due to imperfect (non matched) filtering. When changing to 8PSK we observe an additional 5.5 dB penalty.

Figure 5 (right) shows the measured BER performance of QPSK and 8PSK for quasi-homodyne and intradyne detection. Insertion and coupling losses as well as quantization effects induce an additional penalty of approx. 3 dB in the experiments compared to the simulation. To achieve error free transmission we aim a BER of 10^{-3}, which allows forward error correction codes (FEC) to further decrease the BER. In case of quasi-homodyne detection this threshold is reached for $P_{\mathrm{Rx}} \approx -38$ dBm (QPSK) and $P_{\mathrm{Rx}} \approx -32$ dBm (8PSK). For intradyne detection the threshold is reached for $P_{\mathrm{Rx}} \approx -36.5$ dBm (QPSK) and $P_{\mathrm{Rx}} \approx -29$ dBm (8PSK). Obviously, we observe a penalty of 1.5 dB (QPSK) and 3 dB (8PSK) between quasi-homodyne and intradyne detection. However, these penalties are not seen in the simulation results in Fig. 5 (left). We assume that the frequency offset estimation might still have some inaccuracy, also affected by temporary laser frequency instabilities, which impairs the receiver performance in the experiments. Nevertheless, the results show the potential of intradyne detection based on digital frequency offset and phase noise compensation.

Finally, as mentioned above, using PDs with $\eta \approx 1$ and applying matched filtering, would result in sensitivities near the shot noise limit. Conventional Costas loop based OPLL techniques are further degraded by 3 dB due to the hybrid. However, it is possible to change the hybrid coupling coefficients, which allows an approximation to true homodyne detection. For example, the balanced power splitting of I and Q (50/50) can be changed, in case of BPSK, to an unbalanced splitting of 90/10. Hence, the penalty reduces from 3 dB to approx. 0.5 dB. Further investigations have to show the impact of such a coupling ratio to the intradyne detection scheme with digital frequency offset compensation.

V. CONCLUSION

We presented simulative and experimental investigations of analog and digital frequency offset compensation for optical coherent inter-satellite communication systems. BER measurements could indicate that software-based intradyne detection can successfully reduce the FO as well as PN. Since adaptation to different modulation formats is much easier, this approach seems to be an attractive alternative to standard OPLL techniques. However, suitable space-qualified DSPs are required in practical OISL systems.

REFERENCES

[1] F. Heine et al., "The European Data Relay System, high speed laser based data links," Proc. ASMS/SPSC, pp. 284-286, Livorno, 2014.
[2] M. Gregory et al., "TESAT laser communication terminal performance results on 5.6 Gbit coherent inter satellite and satellite to ground links," Proc. ICSO 2010, Rhodes, 2010.
[3] F. Derr, "Optical QPSK transmission system with novel digital receiver concept," in Electronics Letters, vol. 27, no. 23, pp. 2177-2179, 1991.
[4] M. Seimetz, High-Order Modulation for Optical Fiber Transmission, Springer, Berlin, 2009.
[5] A. Viterbi et al., "Nonlinear estimation of PSK-modulated carrier phase with application to burst digital transmission," IEEE Transactions on Information Theory, vol. 29, pp. 543-551, 1983.
[6] S. Kay, "A fast and accurate single frequency estimator," IEEE Trans. Acoust., Speech, Signal Processing, vol. 37, no.12, pp. 1987-1990, 1989.
[7] S. Bellini et al., "Digital frequency estimation in burst mode QPSK transmission," in IEEE Transactions on Communications, vol. 38, no. 7, pp. 959-961, 1990.
[8] M. Morelli et al., "Feedforward frequency estimation for PSK: A tutorial review." European Transactions on Telecommunications, vol. 9, no.2, pp. 103-116, 1998.
[9] Y. Cao et al., "Frequency Estimation for Optical Coherent MPSK System Without Removing Modulated Data Phase," in IEEE Photonics Technology Letters, vol. 22, no. 10, pp. 691-693, 2010.